Journal of Biomedical Optics

SPIEDigitalLibrary.org/jbo

Epileptic seizure-induced structural and functional changes in rat femur and tibia bone tissues: a Fourier transform infrared imaging study

Sebnem Garip
Deniz Sahin
Feride Severcan

SPIE

Epileptic seizure-induced structural and functional changes in rat femur and tibia bone tissues: a Fourier transform infrared imaging study

Sebnem Garip,[a,b] Deniz Sahin,[c] and Feride Severcan[d]
[a]Middle East Technical University, Department of Biochemistry, 06531 Ankara, Turkey
[b]Istanbul Kemerburgaz University, Department of Medical Biochemistry, Faculty of Medicine, 34217 Istanbul, Turkey
[c]Kocaeli University, Department of Physiology, Faculty of Medicine, Kocaeli, Turkey
[d]Middle East Technical University, Department of Biological Sciences, 06531 Ankara, Turkey

Abstract. The disease- and drug-related bone disorders are rapidly increasing in the population. It is previously reported that anti-epileptic drugs (AEDs) may cause osteopenia, osteoporosis, and fractures in epilepsy patients. However, it cannot be determined whether the bone disorders in epileptic patients are due to AED therapy and/or to epilepsy and epileptic seizures. There is no study in the literature which investigates the sole effects of epilepsy and epileptic seizures on bone tissues. The current study provides the first report on determination of the possible effects of epilepsy and epileptic seizures on long bone tissues. Wistar Albino Glaxo/Rijswijk rats, which are accepted as genetic rat models for human absence epilepsy, were compared with the healthy Wistar rats to get information about the sole effects of epilepsy and epileptic seizures on bones. Cortical regions of tibia and femur bones were studied by Fourier transform infrared microspectroscopy (FTIRM). According to FTIRM parameters, variation on bone mineral and matrix composition, including decreased mineral content, decreased collagen cross-links, increased carbonate substitution, and larger crystals in epileptic group compared to the healthy one, show severe effects of epilepsy and seizures on bone tissues for the first time.
[DOI: 10.1117/1.JBO.18.11.111409]

Keywords: absence epilepsy rat model; bone; bone disorders; Fourier transform infrared imaging; mineral content; carbonate substitution; collagen cross-links; crystallinity.

Paper 130219SSR received Apr. 9, 2013; revised manuscript received Jun. 28, 2013; accepted for publication Jul. 2, 2013; published online Jul. 25, 2013.

1 Introduction

The health and integrity of bone are prerequisite for pain-free movement and have a major impact on the quality of life.[1] Beyond the age-related changes on bone tissues, the disease- and drug-related bone disorders are rapidly increasing in the population. The long term use of anti-epileptic drugs (AEDs) in patients who have epileptic seizures has been associated with alterations in bone mineral density (BMD).[2] The fracture risk of the epileptic population is approximately twice that of the general population, independent of seizure-related falls.[3] The risk was more pronounced in those who used enzyme-inducing AEDs such as phenytoin, phenobarbital, and carbamazepine than in those who used noninducing drugs including lamotrigine and levetiracetam.[4] Previous studies with enzyme-inducing AEDs reported drug-associated osteopenia, osteoporosis, and fractures in epilepsy patients.[5–15] These findings are further supported by studies evaluating the effect of enzyme-inducing AEDs on the expression of specific cytochrome P450 (CYP) isozymes involved in vitamin D metabolism.[16,17] There are, however, some studies contradicting this hypothesis. In these studies, it was reported that serum 25-hydroxyvitamin D levels and/or BMD values, when compared among groups of patients treated with either enzyme-inducing AEDs or nonenzyme-inducing AEDs, did not differ.[6,18–24] Thus, the exact mechanism of pathological changes in bone tissues of epileptic patients is still not clearly understood. Moreover, it could not be determined whether the bone disorders in epileptic patients are due to AED therapy and/or to epilepsy and epileptic seizures, since in these referred studies epileptic patients had epileptic seizures while having the AED treatment, simultaneously. The animal studies[25,26] also could not differentiate the side effects of epileptic seizures and AED therapy since used animal models were not appropriate to study the effects of epileptic seizures alone. Consequently, there is no clinical or animal study which investigates only the effect of convulsive epileptic seizures on bone tissues. Therefore, up to now, the effects of epileptic seizures and the effects of AEDs on bone tissues cannot be differentiated yet from each other.

The current study aimed to investigate, for the first time, the sole effects of epilepsy and epileptic seizures on long bone tissues including femur and tibia by Fourier transform infrared microspectroscopy (FTIRM). We used the genetically induced epileptic rat model; Wistar Albino Glaxo/Rijswijk (WAG/Rij rats) which closely resembles the model of genetically induced absence epilepsy in humans[27] among the other models. The advantage of studying with genetically induced epileptic model is that the effects of chemical epileptic agents like pentylenetetrazol are eliminated.

In clinical practice, bone health is assessed by measuring BMD using the dual-energy X-ray absorptiometry (DXA)

Address all correspondence to: Feride Severcan, Middle East Technical University, Department of Biological Sciences, 06531 Ankara, Turkey. Tel: +90-312-210-51-66; Fax: +90-312-210-76-79; E-mail: feride@metu.edu.tr

0091-3286/2013/$25.00 © 2013 SPIE

method.[4] Using this method, adult and pediatric patients with epilepsy receiving AEDs were found to have significantly reduced BMD at multiple bone sites.[28–31] Nevertheless, many aspects of bone strength cannot be explained by bone density alone. For example, in a study of rats, levetiracetam was found to reduce bone strength and bone formation, even through the results of DXA scans were normal.[32] In this study, histomorphological data indicated that the content of cartilage remnants in the metaphysics in LEV-treated animals was greater than those of control rats, suggesting that possibly previously unexplored mechanisms caused bone depletion. Bone mass (bone quantity) measured with DXA only accounts for 60% to 70% of the variation in bone strength, since bone strength and fracture risk are also influenced by parameters of bone quality such as micro-architecture and tissue composition. *In vivo* studies showed that patients with and without osteoporotic fractures could be better separated with parameters of bone architecture than with BMD.[33] Bone structure analysis was, therefore, studied by high resolution cross sectional imaging techniques with the development of multidetector computed tomography (MD-CT) scanners. With this technique, higher spatial resolution and better depiction of the trabecular bone structure *in vivo* became available.[34,35] One of the main limitations of this technique is the link between spatial resolution and radiation exposure. The higher the spatial resolution of images required, the greater the exposure to radiation. This limits clinical applicability of MD-CT for imaging of the spine and hip.[36] As a recent technique, magnetic resonance imaging (MRI) has tremendous potential for researches in bone diseases.[1] In contrast to CT, MRI does not use ionizing radiation.[36] The main limitation of MRI is that obtaining images *in vivo* with a suitable spatial resolution is still challenging.[1]

In recent years, new specialized noninvasive and/or nondestructive imaging techniques, such as vibrational microspectroscopic techniques, are able to provide information about composition and physical/chemical environment of important bone constituents without any staining processes.[37] Vibrational spectroscopy has been used extensively for getting molecular structure information about mineralized and nonmineralized connective tissues such as bone and cartilage.[38–43] Since, almost all bone disorders will result in composition abnormalities, vibrational microspectroscopy including FTIR microscopy may have an important role as an early diagnostic tool.[37,44] In order to obtain spatially resolved information, FTIRM and Fourier transform infrared imaging (FTIRI) have previously been used to examine bone tissue during aging[45–47] and in osteoporosis,[48–51] osteoarthritis,[52] osteopetrosis,[53] osteomalacia,[54] and osteogenesis imperfect.[55]

In the current study, FTIRM was used to get highly resolved information on the amount of mineral, crystallinity, and collagen properties of bone[53,56,57] while investigating the effects of epilepsy and epileptic seizures on bone tissues. These data may shed light on the prevention of bone disorders in epileptic individuals.

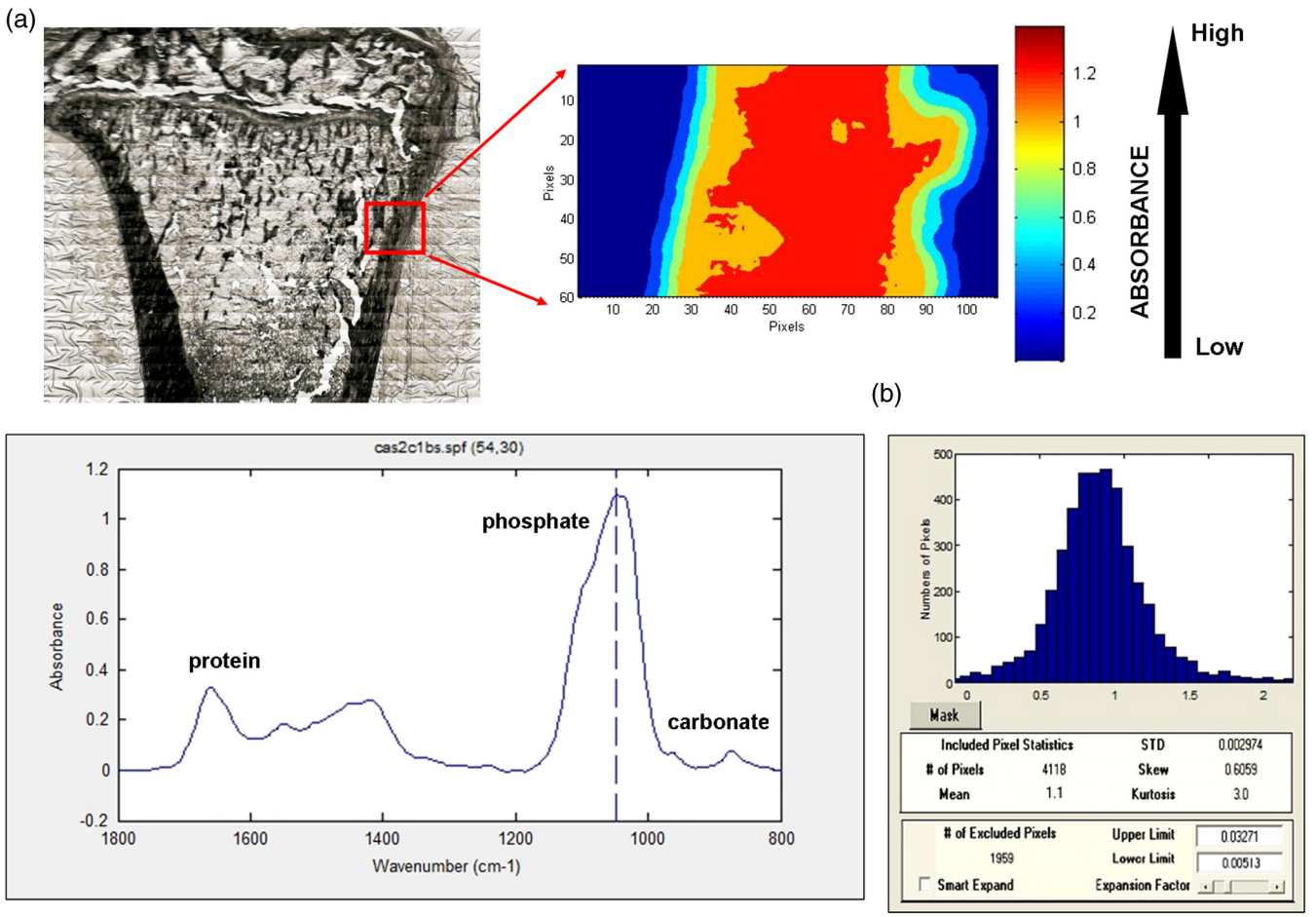

Fig. 1 (a) Representative view of a typical rat tibia bone with a label indicating cortical site examined by FTIRM (c, cortical) and typical FTIR image of the phosphate distribution before spectral processing from cortical site shown in rectangle. (b) The pixel histogram for the image shown in (a).

2 Materials and Methods

2.1 *Animal Studies*

Genetically absence epileptic rats (WAG/Rij) and as a control healthy rats (Wistar rats) were used. Six-month male rats with a mean body weight of 250 to 350 g represent adults as they reach skeletal maturity by approximately 7 to 8 months, and peak bone mass by 1 year of age.[58,59] Rats were kept on a standard pellet diet and given water. Temperature, humidity, and air exchange rate were regulated with a 12-h night and day cycle. The laboratory populations of WAG/Rij rats were preliminary screened for audiogenic susceptibility and animals displaying sound-induced running convulsions (susceptible to audiogenic kindling) were grouped ($n = 6$ for each group).

The animal groups are:

Group 1: Wistar healthy control and
Group 2: WAG/Rij epileptic (absence epilepsy + convulsive seizures).

The comparison of epileptic rats (WAG/Rij) with control healthy rats (Wistar) gives information about the effects of epilepsy and epileptic seizures alone. As a control group, Wistar healthy rats can be used since there are no baseline differences between these two groups except an unknown inherited mutation which induces absence epilepsy.[60,61]

2.2 *Electroencephalographic (EEG) Recording*

To test audiogenic susceptibility each animal was placed into a box ($60 \times 60 \times 60$ cm^3) and a standard complex (multipeak) sound ("keys ringing")[62] produced by a vibro device, with a frequency range of 13 to 85 kHz (maximum of the spectrum in 20 to 40 kHz) and mean intensity of 50 to 60 dB was presented to the rat (for 1.5 min). The manifestation of absence epilepsy in WAG/Rij rats, spike–wave discharges, was monitored in male adult WAG/Rij rats susceptible and not susceptible to audiogenic convulsions. For this purpose, EEG tripolar record electrodes were placed on the cortex surface under anesthetic conditions with ketamine and chloropromazin. Cortical electrodes were located on frontal regions and parietal regions. Reference electrodes were placed on the cerebellum. After a week, the rats were taken into pleksiglas cage and the EEG records were done during seizures and after seizures for 30 min.

All the rats were exposed to the sound stimulation once a day for 5 weeks and EEG records were taken during seizures and after seizures. At the end of the 5 weeks, rats were decapitated and the bone tissues (femur and tibia) were removed and stored at −80°C until FTIRI experiments.

2.3 *Sample Preparation for FTIRM*

Bone tissues; distal femur, and proximal tibia (close parts to knee) were used for the studies with FTIRM. The six tibia and femur bone samples per group were cleaned with soft tissue and were partially fixed in different percentages of ethanol, dehydrated through a series of ethanol, and acetone gradients, and embedded in polymethylmethacrylate (PMMA). Preparation of embedding medium PMMA was done according to methacrylate method.[63] Longitudinal nondecalcified sections of the bone tissues (three sections per bone) were cut by a microtome at 2 μm thickness and mounted on IR transparent, 1 mm thick × 13 mm diameter BaF_2 infrared windows (Spectral Systems, Hopewell Junction, NY) for FTIRM studies.

2.4 *Data Acquisition, Microspectroscopic Measurements and Data Analysis*

In FTIRM studies, Perkin-Elmer Spectrum One/Spotlight 400 Fourier Transform IR Microspectrometer (Perkin-Elmer Corp., Sheldon, CT) was used to map bone sections. For each tissue section, an IR image was obtained with a pixel resolution of 6.25×6.25 μm^2 using a liquid nitrogen cooled mercury cadmium telluride detector. IR spectra were collected in transmission mode from 2000 to 800 cm^{-1} with a spectral resolution of 4 cm^{-1} and with 100 numbers of scans. A spectrum of an area containing no tissue was recorded as a background spectrum. IR data were collected from cortical part of bones. For each animal, three maps were recorded from randomly chosen different regions of cortical parts of bone. Since we have six animals for each group, 18 different maps were used to calculate the IR parameters for each control and epileptic groups.

ISys software (Spectral Dimensions, Olney, MD) was used to analyze the FTIR microspectroscopic data. Whole baseline correction was performed between 2000 and 800 cm^{-1} region in FTIRM studies. After spectral subtraction of embedding medium (PMMA), spectral masking was applied to get rid of the contributions from the nonbone parts on the sections by marking the bone samples. The chemical maps were constructed for each group by taking the ratio of the area and intensity values of specifically selected spectral bands arisen from mineral, matrix, collagen, and carbonate. The area under the bands reflects the concentration of the related molecules.[39,64] Spectral analyses were performed using the ratios of different functional groups such as mineral/matrix ratio, carbonate/phosphate ratio, carbonate/amide I ratio, crystallinity, and collagen cross-link ratio to eliminate the artifacts due to the variations in section thickness. Mineral/matrix ratio was calculated by taking the ratio of the integrated areas of the $v1$, $v3$ phosphate band (1200 to 900 cm^{-1}) to amide I (1720 to 1590 cm^{-1}).[43,65] Carbonate/phosphate ratio was obtained by taking the ratio of the integrated areas of carbonate (890 to 850 cm^{-1}) to $v1$, $v3$ phosphate (1200 to 900 cm^{-1}) band. Collagen cross-link ratio was calculated by taking the ratio of the intensities of two sub-bands under the amide I band. The intensity ratio of the sub-bands at 1660 and 1690 cm^{-1} is related to the relative amount of nonreducible (mature) to reducible (immature) types of cross-links.[50] Crystallinity was estimated from the intensity ratios of sub-bands at 1030 (stoichiometric apatite) and 1020 cm^{-1} (nonstoichiometric apatite).[39,65]

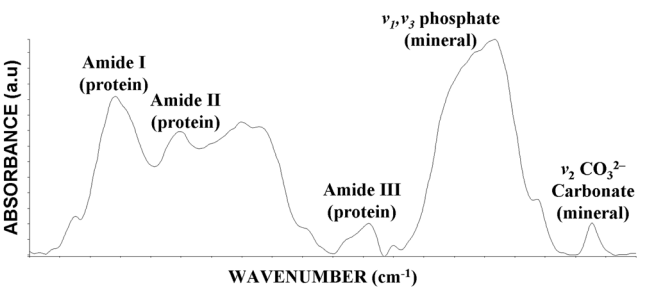

Fig. 2 The average spectra of the control femur bone in 1800 to 800 cm^{-1} region.

The FTIRM results were expressed as representative color-coded images for each parameter and histograms which describe the pixel distribution, mean values and standard deviations (SDs) of the pixel distributions (Fig. 1). Pixel histograms show the average value and heterogeneity of each of the measured parameter. As the parameter values decrease, the pixel distribution in the histograms of these parameters slides to the left side. Not only the changes in mean values, but also the differences in heterogeneity may give important information about the effects of diseases.

2.5 *Statistics*

Statistical analysis was performed by using the SPSS for windows (version 13.0) statistical package (SPSS Inc., Chicago, IL). After testing data for normal distribution and homogeneity of the variance, the FTIRM results for each group expressed as color-coded images and pixel population means were compared with the one-way analysis of variance with a Bonferroni post-hoc test to highlight significant differences between the groups. The results were expressed as mean ± SD. The p values less

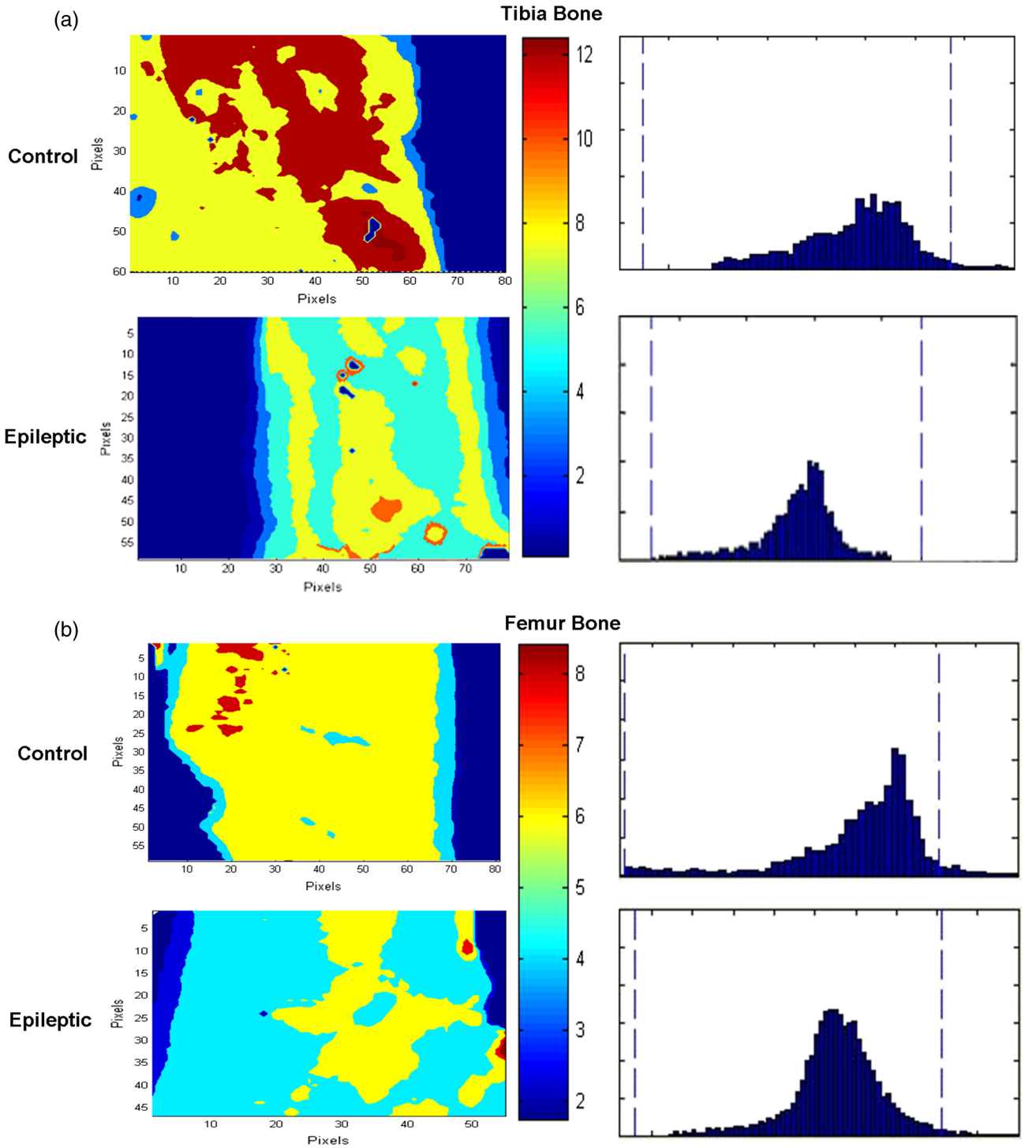

Fig. 3 Typical FTIR images and the pixel histograms of mineral/matrix ratio in cortical sites of (a) tibia and (b) femur bones for control and epileptic group. Color bars represent the scales for each of the parameters. Axes are in pixels, where 1 pixel is 6.25 μm.

than or equal to 0.05 were considered as statistically significant (*$p \leq 0.05$; **$p \leq 0.01$; ***$p \leq 0.001$).

3 Results

The present study is addressed to investigate the possible effects of epilepsy and epileptic seizures on bone tissues of genetically epileptic rats.

Figure 2 shows a typical FTIR spectrum of a rat femur in the 2000 to 800 cm^{-1} region. The main bands and specific assignments of these spectral bands are labeled in the figure.

The overall level of mineralization can be estimated by mineral/matrix ratio ($v1$, $v3$ phosphate/amide I).[43,65] Representative images for mineral/matrix ratio and typical pixel histograms of respective images for tibia and femur bone tissues are presented in Fig. 3(a) and 3(b). This ratio was significantly decreased in epileptic group compared to the healthy control in the cortical parts of both tibia and femur bone tissues (Table 1). This decrease was also seen from the pixel distributions of mineral/matrix parameter in the histograms which were slided to the left side when compared with the control groups [Fig. 3(b)]. As seen from the figures, in both control and epileptic groups, mineral distribution was different in middle and side parts (periosteum and endosteum) of bones. Moreover, both from the images and histograms, it could be observed that there was a higher heterogeneity for mineral content in control groups than in epileptic ones.

Another calculated parameter is carbonate/phosphate ratio which is related to the chemically determined extent of carbonate substitution for phosphate or hydroxide in the mineral crystals.[62,66] The carbonate/phosphate peak area ratio was significantly decreased relative to the healthy control in both tibia and femur bone tissues of epileptic group [Fig. 4(a) and 4(b), Table 1]. The decrease in relative carbonate value was also seen from the pixel distributions in the histograms which were slided to the left side of the histogram [Fig. 4(b)].

It is expected that, while there is a decrease in phosphate content in hydroxyapatite (HA) crystals, the carbonate content which substitutes for phosphate or hydroxide in the mineral crystals would increase. However, according to the carbonate/phosphate ratio, our results revealed a decrease in carbonate content. This controversial finding about carbonate content was further examined to obtain information about changes in the relative ratios of different types of carbonate ion present in bone mineral. Carbonate can substitute for either the hydroxyl group (A type) or the phosphate group (B type), or it can exist on the surface (labile-L type) of the bone apatite crystals.[67–69] The $v2$ CO_3^{2-} region (890 to 850 cm^{-1}) was decomposed into three sub-bands. A band at 866 cm^{-1} is assigned to labile (L type) carbonate, and two bands at 872 and 876 cm^{-1} are assigned to B type and A type carbonates, respectively.[50] In order to determine the changes of these three types of carbonate, we estimated the ratio of the intensity of each component with respect to the amide I band (Table 2). In both tibia and femur bone tissues, B type carbonate which substitutes for phosphate group in the crystals, significantly increased in epileptic groups (Table 2). Since, the B type carbonate which substitutes for phosphate in the mineral crystals, increased, while the A type and L type carbonate significantly decreased in epileptic group relative to the control group, this may be the explanation for the decrease in total carbonate content in the bones. Although mean value of carbonate substitution was significantly different between control and epileptic groups in femur and tibia bones, there was no alteration in heterogeneity of this parameter between two groups as seen from Fig. 4.

The organic matrix of bone is mainly type I collagen. The distinct features of bone (type I) collagen are its cross-linking chemistry and molecular packing structure.[69] An IR parameter, called collagen cross-links, is related to the maturity of the collagen fibrils[65,70] and to the extent of collagen cross-linking in the section being examined. A significant decrease in collagen cross-links in all bone tissues of epileptic groups relative to the control ones was observed [Fig. 5(a) and 5(b), Table 1]. The severe decrease in the cortical parts of tibia and femur bones could also be seen from the pixel distributions of this value which slided to the left side (to the lower values) of the histogram in epileptic group [Fig. 5(b)]. As seen from the figures and histograms, there was a reduction in heterogeneity of collagen cross-link parameter in epileptic groups when compared to control groups.

Table 1 Calculated parameters for FTIRM data of the control ($n = 6$) and epileptic ($n = 6$) groups. p values less than or equal to 0.05 were considered as statistically significant.

	Ratio	Control	Epileptic	p value
Tibia	Mineral/matrix	10.0 ± 0.7	8.0 ± 0.4	<0.01*
	Carbonate/mineral	0.021 ± 0.0000	0.018 ± 0.000	<0.01**
	Collagen cross-links	0.28 ± 0.02	0.24 ± 0.03	<0.05**
	Crystallinity	0.19 ± 0.02	0.24 ± 0.03	<0.001***
Femur	Mineral/matrix	6.3 ± 0.3	4.9 ± 0.2	<0.05**
	Carbonate/mineral	0.014 ± 0.0000	0.12 ± 0.0000	<0.05**
	Collagen cross-links	0.33 ± 0.02	0.25 ± 0.01	<0.01*
	Crystallinity	0.14 ± 0.03	0.24 ± 0.01	<0.01*

*$p \leq 0.01$
**$p \leq 0.05$
***$p \leq 0.001$

Mineral crystallinity is a parameter that corresponds to the crystallite size and perfection as determined by X-ray diffraction.[41,48] This parameter significantly increased in both tibia and femur bone tissues for epileptic group compared to the healthy control [Fig. 6(a) and 6(b), Table 1]. The pixel distribution for the crystallinity parameter in the epileptic group was skewed to the right, showing the presence of relatively more large crystals than smaller ones [Fig. 6(b)]. In spite of the significant change in crystallinity mean value, there was no difference in heterogeneity of crystal size between control and epileptic groups as seen from Fig. 6.

As a summary, the epileptic group had lower mineral content and collagen cross-links, and higher B type carbonate substitution and crystallinity value when compared to the healthy rats. Besides

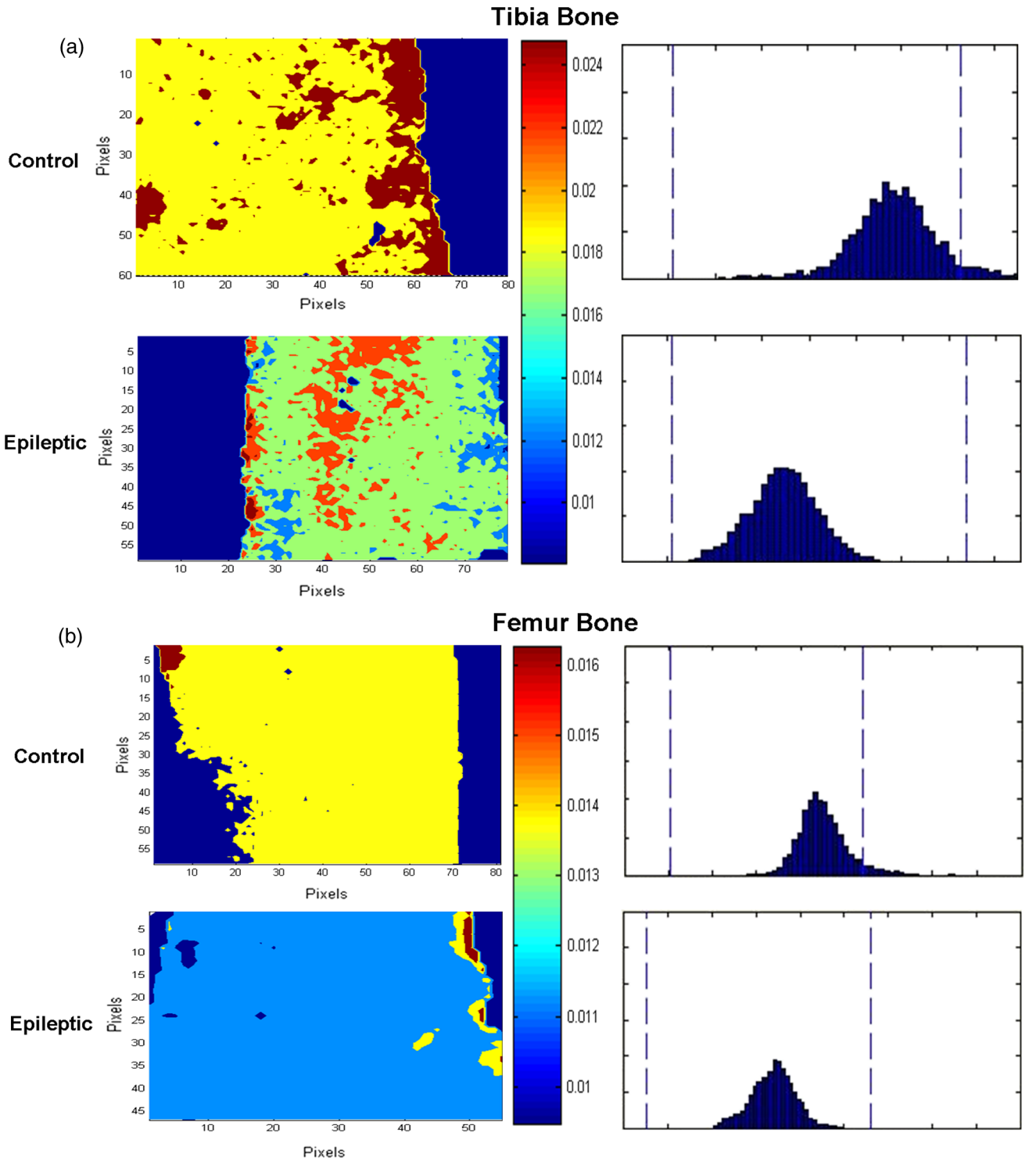

Fig. 4 Typical FTIR images and the pixel histograms of carbonate/phosphate ratio in cortical sites of (a) tibia and (b) femur bones for control and epileptic group. Color bars represent the scales for each of the parameters. Axes are in pixels, where 1 pixel is 6.25 μm.

the differences of mean values for these parameters, there was a reduction in heterogeneity of mineral content and cross-link ratio between control and epileptic groups.

4 Discussion

In the present study, the possible effects of epilepsy and epileptic seizures on bone tissues of genetically epileptic rats were investigated to determine the disease-related structural changes of bones by FTIRM. The current study provides the first report of the effects of epilepsy and epileptic seizures alone on bone tissues of epileptic systems. In this study, we used a genetically epileptic animal model (WAG/Rij rats) which closely resemble the model of genetically induced absence epilepsy in humans[71,72] among the other models. The comparison of epileptic rats with control healthy rats gives information about the effects of epilepsy and epileptic seizures alone.

The properties of bone that determine its mechanical strength are its geometry (shape and connectivity), composition, and material properties.[73] These material properties include mineral content, mineral and matrix composition, cellular activity, and distribution of crystal sizes.[74,75] Most of these material properties with the exception of cellular activity can be determined by infrared microscopy and infrared microscopic imaging.

The mineral content (mineral/matrix ratio) is important for mechanical strength in bones and the decreased content would make the bones weaker.[56] Mineral/matrix ratio calculated by FTIR spectroscopy is directly related to "ash weight," proving a quantitative measurement of the extent of mineralization in the bone.[70,76] In both tibia and femur bones, mineral content drastically decreased in epileptic group. In the previous studies, it was reported that the mineral/matrix ratio, i.e., the mineral content, decreased in osteoporotic tissues.[77,78] In a study with ovariectomized monkeys,[79] it was noted that decreased mineral/matrix ratio is both a characteristic of immature bone and an indication of osteoporosis. It was reported that the significant decrease in mineral/matrix ratio is consistent with the general osteoporotic phenotype which was previously observed by μ-CT analysis.[80,81] Vitamin D deficiency has been linked to the pathogenesis of osteoporosis and fractures.[82] Since, vitamin D is known to regulate collagen synthesis as well as mineral ion transport, and expression of vitamin D-dependent extracellular matrix proteins, all of these may contribute to the observed decreased mineral content in epileptic groups. In the current study, it was also observed that the heterogeneity of mineral content was reduced in epileptic groups compared to the control ones. In a recent study, low heterogeneity of mineral/matrix ratio was reported in fracture cases.[83] An explanation for decreased heterogeneity of mineral content in epileptic bones may be a less actively remodeled tissue compared with controls, possibly associated with reduced osteocyte density adjacent to the canal.[84]

Biological HA is a poorly crystalline carbonate.[49] Although bone contains significantly less carbonate than phosphate, carbonate plays an important role in the dissolution of mineral and the resorption of bone.[50] In the current study, B type carbonate increased in epileptic group while A type and L type (labile) carbonate decreased for all bone tissues. This implies that the carbonate incorporation into the apatite lattice increases. It was previously reported that the carbonate content was higher in the HA crystals in osteoporosis.[76] The observation that B type carbonate content increased in this study suggests that there is either an impaired mineralization due to vitamin D deficiency or excessive bone turnover, while the overall degree of substitution is highly dependent upon many factors, such as bone species, strain, and type.[49] In the previous studies, high carbonate substitution in HA has been linked to increased bone dissolution[85] and osteoclastic resorption[49] and is related to fracture events in iliac crest biopsies.[49] Interest in crystallinity has been long standing because of previously reported tendency for hip fracture cases to develop some very large crystals[86] and the likelihood that such crystals are brittle.[87]

The collagen cross-link network is important for structural and mechanical properties of the bone.[79] Any alteration in this network can result in severe dysfunction of the tissue and it has been suggested that the composition of bone collagen is altered in bone disorders.[78,85,88–90] Intermolecular collagen cross-linking is also important for the development of the underlying matrices that are essential for initial mineral formation and crystal growth. This matrix also contributes to mechanical properties such as tensile strength and viscoelasticity.[78] Our collagen cross-link ratio results demonstrate that collagen cross-links in the bones of epileptic groups decreased compared to the control group. In the study of Viguet-Carrin et al.,[91] it was reported that when the formation of collagen cross-links was chemically inhibited the bone strength decreased despite of "normal mineralization." In a recent study,[92] a condition called homocysteinuria in which homocysteine interferes with collagen cross-link formation was associated with spontaneous bone insufficiency fractures. Moreover, disturbances in the collagen maturation can affect the mineralization process and may lead to bone defects.[43]

HA crystal size provides an important information about the bone structure. As bone ages or matures, crystal size and perfection increase and the apatite environment can become more stoichiometric.[93,94] In the current study, epileptic group had higher 1030/1020 cm^{-1} ratio indicating a greater crystal size and perfection in all bone types. Recent studies[95,96] suggested that osteoporotic patients also contain larger apatite crystals which negatively affect the mechanical properties of bone tissues. It was reported that increased bone mineral particle size is associated with increased bone fragility.[49] Bone mineral crystals are extremely small, inducing a large specific surface of bone crystals, and contributing to an increased quantity of electrostatic bonds between mineral and collagen matrix.

Table 2 A type, B type, and labile (L type) carbonate ratios calculated by taking carbonate/amide I intensity ratio for control ($n = 6$) and epileptic ($n = 6$) groups. p values less than or equal to 0.05 were considered as statistically significant.

	Carbonate type	Control	Epileptic	p value
Tibia	A type	3.23 ± 0.04	3.19 ± 0.02	0.1
	B type	3.70 ± 0.02	3.88 ± 0.03	<0.01**
	L type	3.26 ± 0.03	3.19 ± 0.01	<0.01**
Femur	A type	2.89 ± 0.02	2.84 ± 0.03	0.07
	B type	3.07 ± 0.03	3.17 ± 0.05	<0.05*
	L type	2.09 ± 0.02	2.83 ± 0.02	<0.05*

*$p \leq 0.05$
**$p \leq 0.01$

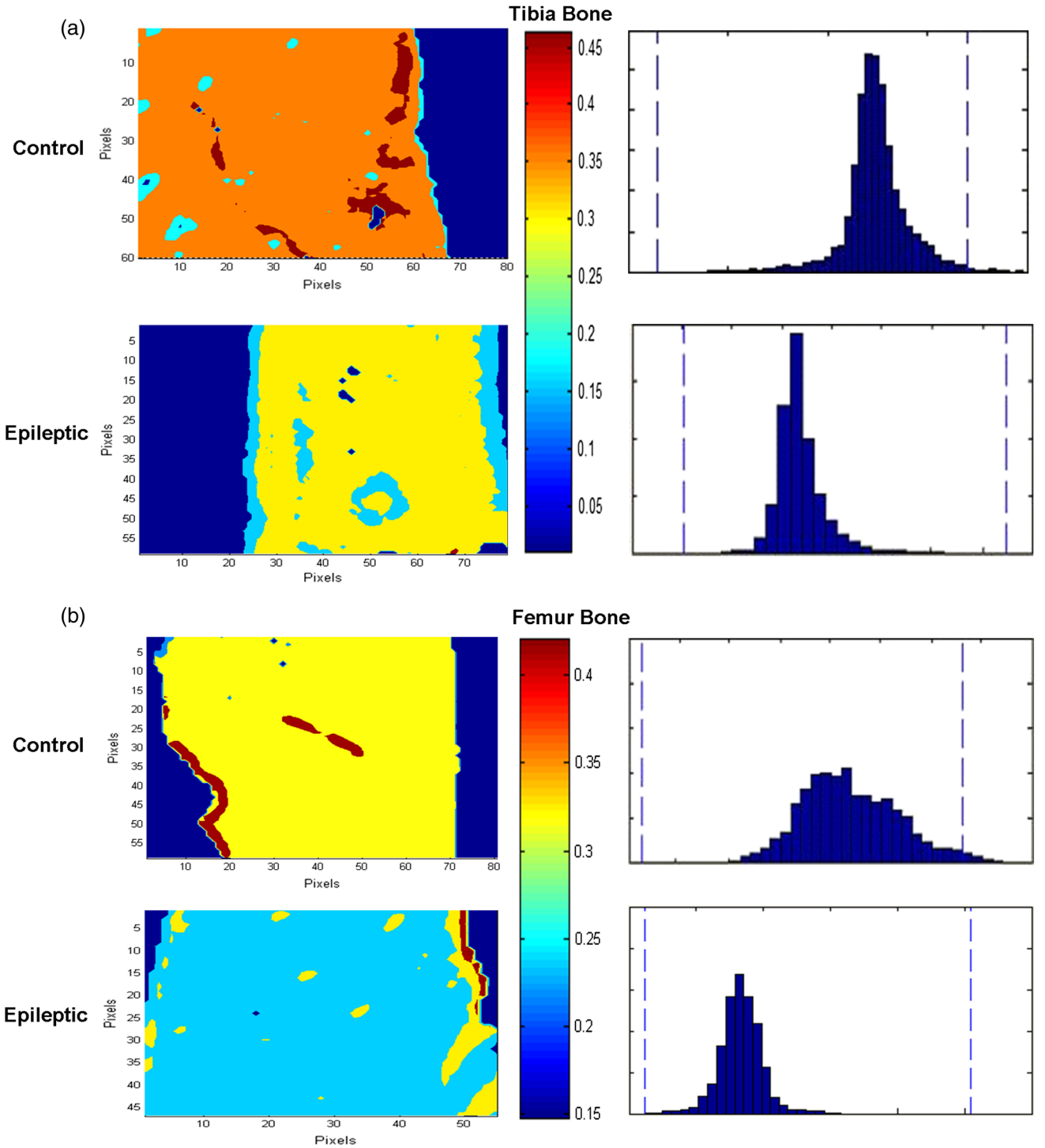

Fig. 5 Typical FTIR images and the pixel histograms of collagen cross-links ratio in cortical sites of (a) tibia and (b) femur bones for control and epileptic group. Color bars represent the scales for each of the parameters. Axes are in pixels, where 1 pixel is 6.25 μm.

Mechanically, the highly ordered location and orientation of very small crystals within the collagen fibrils not only contribute to the rigidity and strength of the bone substance, but their small size also permits an acceptable range of flexibility without fracture or disruption of the bone substance.[97] However, the presence of large crystals decreases the surface area with collagen fibrils and, therefore, does not contribute to mechanical strength.[94,98] In our study, increases in crystal size of epileptic bones may exist because the younger smaller crystals have been excessively resorbed (osteoporosis) or because formation of new mineral is impaired due to vitamin D deficiency and thus the existing crystals grow rather than forming new ones.[99]

In the current study, heterogeneity of mineral content and cross-link ratio was reduced in epileptic groups. In a previous study, osteoporotic patients treated with bisphosphonates are likely to be affected by further reductions in heterogeneity of

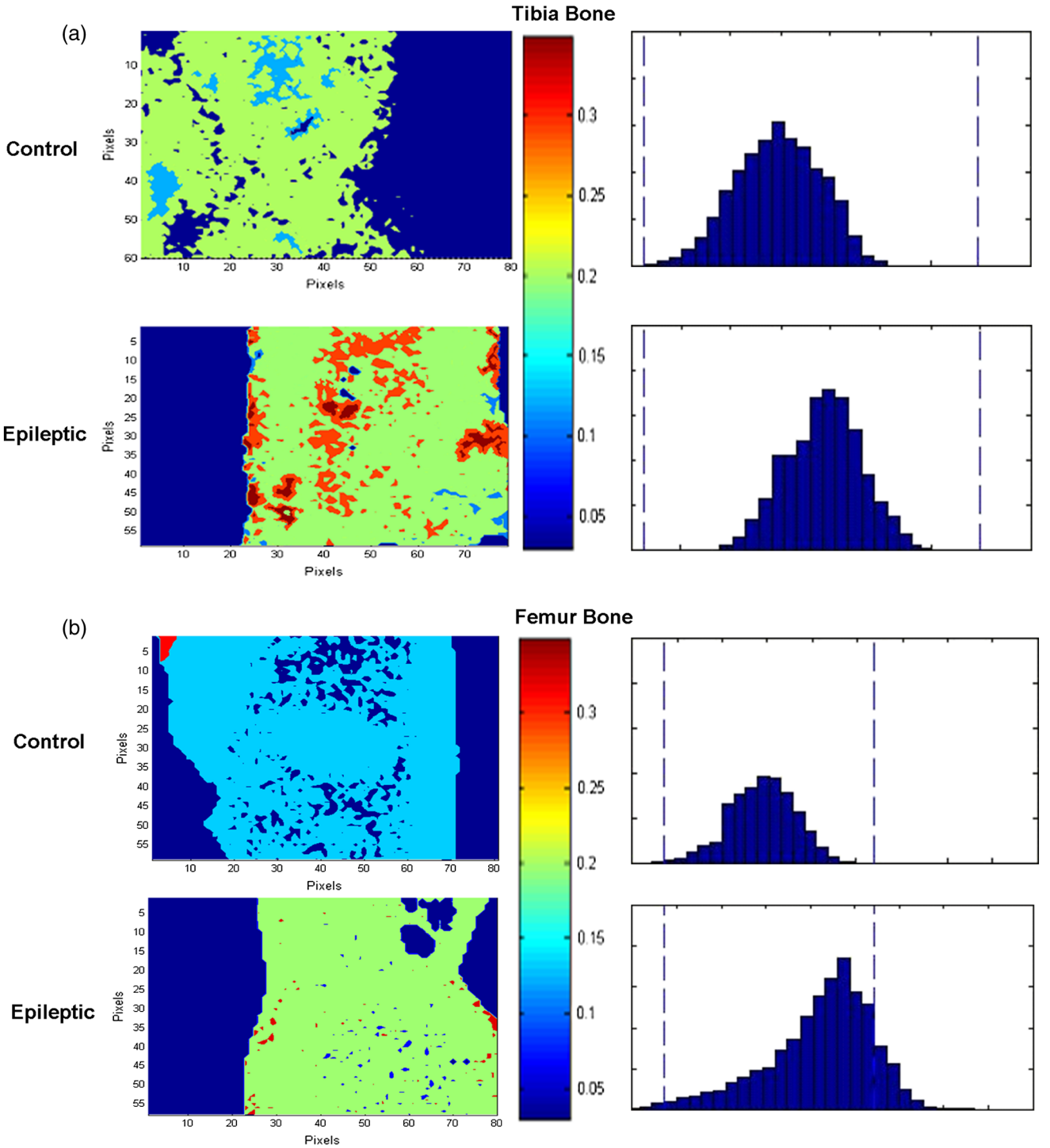

Fig. 6 Typical FTIR images and the pixel histograms of crystallinity ratio in cortical sites of (a) tibia and (b) femur bones for control and epileptic group. Color bars represent the scales for each of the parameters. Axes are in pixels, where 1 pixel is 6.25 μm.

FTIR microspectroscopic parameters.[83] The decrease in bone heterogeneity observed in dog tibias after 1 year's bisphosphonate treatment[51] was used to explain the significant accumulation of microdamage observed in vertebrae of dogs given similar treatments.[100] This association raises the possibility that reduced heterogeneity in disease state is detrimental to bone's toughness. Healthy bone tissue is highly heterogeneous, and there is a evidence that this heterogeneity affects the mechanical properties of the bone material by preventing the proliferation of microcracks.[51]

FTIR microspectroscopy is an emerging and still relatively new technique for diagnosis of musculoskeletal diseases. It has enormous potential for research on bone and its disorders. The current limitation of this technique is the need to isolate the tissues and embedding and sectioning. In the near future, developed fiber optic probes for the use of FTIR to examine the

surface of bone through skin may enable imaging spectroscopy without the need for biopsies.

5 Conclusion

In the current study, the effects of epilepsy and epileptic seizures on tibia and femur tissues of genetically epileptic rats were reported by using FTIR microspectroscopic imaging. Variations on bone mineral and matrix composition (decreased mineral content, larger crystals, increased carbonate substitution, decreased collagen cross-links) in epileptic group compared to the healthy ones may due to the either excessive bone turnover or impaired mineralization due to vitamin D deficiency. In FTIRM studies, according to the degree of variation and significance between the calculated parameter values, the tibia bone tissues were found to be more affected from epilepsy and epileptic seizures than the femur tissues.

Acknowledgments

We are grateful to Dr. Gul Ilbay for her help in animal studies. This study was supported by Middle East Technical University (METU) research fund BAP-07.02.2009.00.01.

References

1. F. Eckstein, D. Burstein, and T. M. Link, "Quantitative MRI of cartilage and bone: degenerative changes in osteoarthritis," *Changes* **19**(7), 822–854 (2006).
2. K. Phabphal et al., "The association between BsmI polymorphism and bone mineral density in young patients with epilepsy who are taking phenytoin," *Epilepsia* **54**(2), 249–255 (2013) .
3. S. J. Petty, T. J. O'Brien, and J. D. Wark, "Anti-epileptic medication and bone health," *Osteoporosis Int.* **18**(2), 129–142 (2007).
4. S. Svalheim et al., "Bone health in adults with epilepsy," *Acta Neurol. Scand., Suppl.* **124**(191), 89–95 (2011).
5. G. Coppola et al., "Bone mineral density in children, adolescents, and young adults with epilepsy," *Epilepsia* **50**(9), 2140–2146 (2009).
6. A. Verrotti et al., "Increased bone turnover in epileptic patients treated with carbamazepine," *Ann. Neurol.* **47**(3), 385–388 (2000).
7. J. Feldkamp et al., "Long-term anticonvulsant therapy leads to low bone mineral density—evidence for direct drug effects of phenytoin and carbamazepine on human osteoblast-like cells," *Exp. Clin. Endocrinol. Diabetes* **108**(1), 37–43 (2000).
8. S. Mintzer et al., "Vitamin D levels and bone turnover in epilepsy patients taking carbamazepine or oxcarbazepine," *Epilepsia* **47**(3), 510–515 (2006).
9. I.-J. Chou et al., "Evaluation of bone mineral density in children receiving carbamazepine or valproate monotherapy," *Acta Paediatr. Taiwan* **48**(6), 317–322 (2007).
10. S. H. Kim et al., "A 6-month longitudinal study of bone mineral density with antiepileptic drug monotherapy," *Epilepsy Behav.* **10**(2), 291–295 (2007).
11. R. Shellhaas and S. M. Joshi, "Vitamin D and bone health among children with epilepsy," *Pediatr. Neurol.* **42**(6), 385–393 (2010).
12. A. Gniatkowska-Nowakowska, "Fractures in epilepsy children," *Seizure* **19**(6), 324–325 (2010).
13. R. Akin et al., "Evaluation of bone mineral density in children receiving antiepileptic drugs," *Pediatr. Neurol.* **19**(2), 129–131 (1998).
14. G. Kafali, T. Erselcan, and F. Tanzer, "Effect of antiepileptic drugs on bone mineral density in children between ages 6 and 12 years," *Clin. Pediatr.* **38**(2), 93–98 (1999).
15. E. Erbayat Altay et al., "Evaluation of bone mineral metabolism in children receiving carbamazepine and valproic acid," *J. Pediatr. Endocrinol. Metab.* **13**(7), 933–939 (2000).
16. J. M. Pascussi et al., "Possible involvement of pregnane X receptor-enhanced CYP24 expression in drug-induced osteomalacia," *J. Clin. Invest.* **115**(1), 177–186 (2005).
17. A. Zhou et al., "Steroid and xenobiotic receptor and vitamin D receptor crosstalk mediates CYP24 expression and drug-induced osteomalacia," *J. Clin. Invest.* **116**(6), 1703–1712 (2006).
18. L. J. Stephen et al., "Bone density and antiepileptic drugs: a case-controlled study," *Seizure* **8**(6), 339–342 (1999).
19. A. Verrotti et al., "Increased bone turnover in prepubertal, pubertal, and postpubertal patients receiving carbamazepine," *Epilepsia* **43**(12), 1488–1492 (2002).
20. A. M. Pack et al., "Bone mass and turnover in women with epilepsy on antiepileptic drug monotherapy," *Ann. Neurol.* **57**(2), 252–257 (2005).
21. P. C. Souverein et al., "Use of antiepileptic drugs and risk of fractures: case–control study among patients with epilepsy," *Neurology* **66**(9), 1318–1324 (2006).
22. I. Tsiropoulos et al., "Exposure to antiepileptic drugs and the risk of hip fracture: a case–control study," *Epilepsia* **49**(12), 2092–2099 (2008).
23. N. Jette et al., "Association of antiepileptic drugs with nontraumatic fractures," *Arch. Neurol. (Chicago)* **68**(1), 107–12 (2011).
24. J. M. Nicholas et al., "Fracture risk with use of liver enzyme inducing antiepileptic drugs in people with active epilepsy: cohort study using the general practice research database," *Seizure* **22**(1), 37–42 (2013) .
25. K. Onodera et al., "Phenytoin-induced bone loss and its prevention with alfacalcidol or calcitriol in growing rats," *Calcif. Tissue Int.* **69**(2), 109–116 (2001).
26. K. Onodera et al., "Effects of phenytoin and/or vitamin K2 (menatetrenone) on bone mineral density in the tibiae of growing rats," *Life Sci.* **70**(13), 1533–1542 (2002).
27. G. Van Luijtelaar and E. Sitnikova, "Global and focal aspects of absence epilepsy: the contribution of genetic models," *Neurosci. Biobehav. Rev.* **30**(7), 983–1003 (2006).
28. A. L. Andress et al., "Antiepileptic drug-induced bone loss in young male patients who have seizures," *Arch. Neurol.* **59**(5), 781–786 (2002).
29. G. Farhat et al., "Effect of antiepileptic drugs on bone density in ambulatory patients," *Neurology* **58**(9), 1348–1353 (2002).
30. H. Tsukahara et al., "Bone mineral status in ambulatory pediatric patients on long-term anti-epileptic drug therapy," *Pediatr. Int.* **44**(3), 247–253 (2002).
31. K. Beerhorst et al., "Antiepileptic drugs and high prevalence of low bone mineral density in a group of inpatients with chronic epilepsy," *Acta Neurol. Scand.* **29**, 1–8 (2013).
32. L. S. H. Nissen-Meyer et al., "Levetiracetam, phenytoin, and valproate act differently on rat bone mass, structure, and metabolism," *Epilepsia* **48**(10), 1850–1860 (2007).
33. J. S. Bauer and T. M. Link, "Advances in osteoporosis imaging," *Eur. J. Radiol.* **71**(3), 440–449 (2009).
34. A. S. Issever et al., "Assessment of trabecular bone structure using MDCT: comparison of 64- and 320-slice CT using HR-pQCT as the reference standard," *Eur. Radiol.* **20**(2), 458–468 (2010).
35. T. M. Link et al., "High-resolution MRI vs multislice spiral CT: which technique depicts the trabecular bone structure best?," *Eur. Radiol.* **13**(4), 663–671 (2003).
36. T. M. Link, "The Founder's lecture 2009: advances in imaging of osteoporosis and osteoarthritis," *Skeletal Radiol.* **39**(10), 943–955 (2010).
37. S. Garip and A. L. Boskey, "Diagnosis of bone and cartilage diseases," in *Vibrational Spectroscopy in Diagnosis and Screening*, F. Severcan and H. I. Parvez, Eds., IOS Press, Amsterdam, Netherlands (2012).
38. S. Garip et al., "Evaluation and discrimination of simvastatin-induced structural alterations in proteins of different rat tissues by FTIR spectroscopy and neural network analysis," *Analyst* **135**(12), 3233–3241 (2010).
39. S. Garip and F. Severcan, "Determination of simvastatin-induced changes in bone composition and structure by Fourier transform infrared spectroscopy in rat animal model," *J. Pharm. Biomed. Anal.* **52**(4), 580–588 (2010).
40. A. L. Boskey, L. Spevak, and R. S. Weinstein, "Spectroscopic markers of bone quality in alendronate-treated postmenopausal women," *Osteoporosis Int.* **20**(5), 793–800 (2009).
41. F. Severcan et al., "Effects of in-office and at-home bleaching on human enamel and dentin: an in vitro applications of Fourier transform infrared study," *Appl. Spectrosc.* **62**(11) 1274–1279 (2008).

42. A. M. Misof et al., "Differential effects of alendronate treatment on bone from growing osteogenesis imperfecta and wild-type mouse," *Bone* **36**(1), 150–158 (2005).
43. H. Boyar et al., "The effects of chronic hypoperfusion on rat cranial bone mineral and organic matrix. A Fourier transform infrared spectroscopy study," *Anal. Bioanal. Chem.* **379**(3), 433–438 (2004).
44. A. Carden and M. D. Morris, "Application of vibrational spectroscopy to the study of mineralized tissues (review)," *J. Biomed. Opt.* **5**(3), 259–268 (2000).
45. M. E. Faillace, R. J. Phipps, and L. M. Miller, "Fourier transform infrared imaging as a tool to chemically and spatially characterize matrix-mineral deposition in osteoblasts," *Calcif. Tissue Int.* **92**(1), 50–58 (2013) .
46. L. M. Miller et al., "Accretion of bone quantity and quality in the developing mouse skeleton," *J. Bone Miner. Res.* **22**(7), 1037–1045 (2007).
47. A. Busa et al., "Rapid establishment of chemical and mechanical properties during lamellar bone formation," *Calcif. Tissue Int.* **77**(6), 386–394 (2005).
48. A. L. Boskey et al., "Comparison of mineral quality and quantity in iliac crest biopsies from high- and low-turnover osteoporosis: an FT-IR microspectroscopic investigation," *Osteoporosis Int.* **16**(12), 2031–2038 (2005).
49. S. Gourion-Arsiquaud et al., "Use of FTIR spectroscopic imaging to identify parameters associated with fragility fracture," *J. Bone Miner. Res.* **24**(9), 1565–1571 (2009).
50. R. Y. Huang et al., "In situ chemistry of osteoporosis revealed by synchrotron infrared microspectroscopy," *Bone* **33**(4), 514–521 (2003).
51. A. Donnelly et al., "Reduced cortical bone compositional heterogeneity with bisphosphonate treatment in postmenopausal women with intertrochanteric and subtrochanteric fractures," *J. Bone Miner. Res.* **27**(3), 672–678 (2012).
52. L. M. Miller et al., "Alterations in mineral composition observed in osteoarthritic joints of cynomolgus monkeys," *Bone* **35**(2), 498–506 (2004).
53. A. Boskey and N. Pleshko Camacho, "FT-IR imaging of native and tissue-engineered bone and cartilage," *Biomaterials* **28**(15), 2465–2478 (2007).
54. A. Faibish et al., "Infrared imaging of calcified tissue in bone biopsies from adults with osteomalacia," *Bone* **36**(1), 6–12 (2005).
55. K. Lindahl et al., "COL1 C-propeptide cleavage site mutations cause high bone mass osteogenesis imperfecta," *Hum. Mutat.* **32**(6), 598–609 (2011).
56. Y. Ling et al., "DMP1 depletion decreases bone mineralization in vivo: an FTIR imaging analysis," *J. Bone Miner. Res.* **20**(12), 2169–2177 (2005).
57. A. Boivin et al., "The role of mineralization and organic matrix in the microhardness of bone tissue from controls and osteoporotic patients," *Bone* **43**(3), 532–538 (2008).
58. M. M. Brzóska and J. Moniuszko-Jakoniuk, "Low-level lifetime exposure to cadmium decreases skeletal mineralization and enhances bone loss in aged rats," *Bone* **35**(5), 1180–1191 (2004).
59. M. J. Jayo et al., "Effects of an oral contraceptive combination with or without androgen on mammary tissues: a study in rats," *J. Soc. Gynecol. Invest.* **7**(4), 257–265 (2000).
60. B. S. Naquet and R. Meldrum, "Effects of psilocybin, dimethyltryptamine, mescaline and various lysergic acid derivatives on the EEG and on photically induced epilepsy in the baboon (Papio papio)," *Electroencephalogr. Clin. Neurophysiol.* **31**(6), 563–572 (1971).
61. A. M. Coenen et al., "Genetic models of absence epilepsy, with emphasis on the WAG/Rij strain of rats," *Epilepsy Res.* **12**(2), 75–86 (1992).
62. L. V. Krushinski, L. N. Molodkina, and D. Fless, "The functional studies of the brain during sonic stimulation," in *Physiological Effects of Noise*, B. L. Welch, Eds., pp. 159–183, Plenum Press, New York, NY (1978).
63. R. G. Erben, "Embedding of bone samples in methylmethacrylate: an improved method suitable for bone histomorphometry, histochemistry, and immunohistochemistry," *J. Histochem. Cytochem.* **45**(2), 307–313 (1997).
64. C. Aksoy et al., "Bone marrow mesenchymal stem cells in patients with beta thalassemia major: molecular analysis with attenuated total reflection-Fourier transform infrared spectroscopy study as a novel method," *Stem Cells Dev.* **21**(11), 2000–2011 (2012).
65. S. Gourion-Arsiquaud et al., "Fourier transform infrared imaging of femoral neck bone: reduced heterogeneity of mineral-to-matrix and carbonate-to-phosphate and more variable crystallinity in treatment-naive fracture cases compared with fracture-free controls," *J. Bone Miner. Res.* **28**(1), 150–161 (2013) .
66. F. Calton, J. Macleay, and A. L. Boskey, "Fourier transform infrared imaging analysis of cancellous bone in alendronate- and raloxifene-treated osteopenic sheep," *Cells Tissues Organs* **194**(2–4), 302–306 (2011).
67. C. P. Jerome et al., "The androgenic anabolic steroid nandrolone decanoate prevents osteopenia and inhibits bone turnover in ovariectomized cynomolgus monkeys," *Bone* **20**(4), 355–364 (1997).
68. N. P. Camacho et al., "Complementary information on bone ultrastructure from scanning small angle X-ray scattering and Fourier-transform infrared microspectroscopy," *Bone* **25**(3), 287–293 (1999).
69. K. Nagata, "HSP47 as a collagen-specific molecular chaperone: function and expression in normal mouse development," *Semin. Cell Dev. Biol.* **14**(5), 275–282 (2003).
70. A. L. Boskey and R. Mendelsohn, "Infrared spectroscopic characterization of mineralized tissues," *Vib. Spectrosc.* **38**(1–2), 107–114 (2005).
71. M. L. Coenen and E. L. J. M. Van Luijtelaar, "Genetic animal models for absence epilepsy: a review of the WAG/Rij strain of rats," *Behav. Genet.* **33**(6), 635–655 (2003).
72. I. S. Midzyanovskaya et al., "Mixed forms of epilepsy in a subpopulation of WAG/Rij rats," *Epilepsy Behav.* **5**(5), 655–661 (2004).
73. M. L. Bouxsein, "Non-invasive measurements of bone strength: promise and peril," *J. Musculoskelet. Neuronal. Interact.* **4**(4), 404–405 (2004).
74. R. D. Blank et al., "Spectroscopically determined collagen Pyr/deH-DHLNL cross-link ratio and crystallinity indices differ markedly in recombinant congenic mice with divergent calculated bone tissue strength," *Connect. Tissue Res.* **44**(3–4), 134–142 (2003).
75. A. L. Boskey, "Mineralization of Bones and Teeth," *Elements* **3**(6), 385–391 (2007).
76. D. Faibish, S. M. Ott, and A. L. Boskey, "Mineral changes in osteoporosis: a review," *Clin. Orthop. Relat. Res.* **443**, 28–38 (2006).
77. S. J. Gadaleta et al., "Fourier transform infrared spectroscopy of the solution-mediated conversion of amorphous calcium phosphate to hydroxyapatite: new correlations between X-ray diffraction and infrared data," *Calcif. Tissue Int.* **58**(1), 9–16 (1996).
78. D. J. Leeming et al., "Is bone quality associated with collagen age?," *Osteoporosis Int.* **20**(9), 1461–1470 (2009).
79. S. Bohic et al., "Characterization of the trabecular rat bone mineral: effect of ovariectomy and bisphosphonate treatment," *Bone* **26**(4), 341–348 (2000).
80. Y. Ueki et al., "Increased myeloid cell responses to M-CSF and RANKL cause bone loss and inflammation in SH3BP2 'cherubism' mice," *Cell* **128**(1), 71–83 (2007).
81. A. J. Wang et al., "Pro416Arg cherubism mutation in Sh3bp2 knock-in mice affects osteoblasts and alters bone mineral and matrix properties," *Bone* **46**(5), 1306–1315 (2010).
82. N. Binkley, D. Krueger, and G. Lensmeyer, "25-hydroxyvitamin D measurement, 2009: a review for clinicians," *J. Clin. Densitom.* **12**(4), 417–427 (2009).
83. S. Gourion-Arsiquaud et al., "Fourier transform infrared imaging of femoral neck bone: reduced heterogeneity of mineral-to-matrix and carbonate-to-phosphate and more variable crystallinity in treatment-naive fracture cases compared with fracture-free controls," *J. Bone Miner. Res.* **28**(1), 150–161 (2013) .
84. J. Power et al., "Osteocyte recruitment declines as the osteon fills in: interacting effects of osteocytic sclerostin and previous hip fracture on the size of cortical canals in the femoral neck," *Bone* **50**(5), 1107–1114 (2012).
85. R. Z. LeGeros et al., "Synergistic effects of magnesium and carbonate on properties of biological and synthetic apatites," *Connect. Tissue Res.* **33**(1–3), 203–209 (1995).
86. P. Augat and S. Schorlemmer, "The role of cortical bone and its microstructure in bone strength," *Age Ageing* **35**(Suppl. 2), ii27–ii31 (2006).
87. A. Gao et al., "Materials become insensitive to flaws at nanoscale: lessons from nature," *Proc. Natl. Acad. Sci. U. S. A.* **100**(10), 5597–5600 (2003).
88. K. Otsubo et al., "Cross-linking connectivity in bone collagen fibrils: the COOH-terminal locus of free aldehyde," *Biochemistry* **31**(2), 396–402 (1992).

89. L. Knott et al., "Biochemical changes in the collagenous matrix of osteoporotic avian bone," *Biochem. J.* **310**(Pt 3), 1045–1051 (1995).
90. L. Knott and A. J. Bailey, "Collagen cross-links in mineralizing tissues: a review of their chemistry, function, and clinical relevance," *Bone* **22**(3), 181–187 (1998).
91. S. Viguet-Carrin, P. Garnero, and P. D. Delmas, "The role of collagen in bone strength," *Osteoporosis Int.* **17**(3), 319–336 (2006) .
92. R. Levasseur, "Bone tissue and hyperhomocysteinemia," *Jo. Bone Spine* **76**(3), 234–240 (2009).
93. A. B. Barry et al., "Effect of age on rat bone solubility and crystallinity," *Calcif. Tissue Int.* **71**(2), 167–171 (2002).
94. A. Farlay et al., "Mineral maturity and crystallinity index are distinct characteristics of bone mineral," *J. Bone Miner. Metab.* **28**(4), 433–445 (2010).
95. M. A. Rubin et al., "TEM analysis of the nanostructure of normal and osteoporotic human trabecular bone," *Bone* **33**(3), 270–282 (2003).
96. C.-L. Benhamou, "Effects of osteoporosis medications on bone quality," *Jo. Bone Spine* **74**(1), 39–47 (2007).
97. W. J. Landis, "The strength of a calcified tissue depends in part on the molecular structure and organization of its constituent mineral crystals in their organic matrix," *Bone* **16**(5), 533–544 (1995).
98. A. Chachra et al., "The effect of fluoride treatment on bone mineral in rabbits," *Calcif. Tissue Int.* **64**(4), 345–351 (1999).
99. A. Said et al., "Mandibular bone alterations of ovariectomized rats under vitamin D insufficiency," *Histol. Histopathol.* **23**(4), 479–485 (2008).
100. M. R. Allen et al., "Raloxifene enhances vertebral mechanical properties independent of bone density," *Bone* **39**(5), 1130–1135 (2006).